The possibility of lasers based on the innershell transitions of Ne-like and Ni-like ions

Elena Ivanova, Larry Knight

Brigham Young University, ESC, Provo, Utah, 84204

ABSTRACT

Our earlier papers [1,2] showed that laser gain is possible on the innershell 2s-2p transitions of Ne-like ions. This result was confirmed by more comprehensive calculations[3]. In more recent works[4-5] it was shown that laser gain is also possible on transitions between highly excited states. We summarize these results and present atomic-kinetic calculations for gain values along the Ne-like sequence for argon, iron, krypton, silver and xenon. For these ions the optimum plasma conditions are found for all possible laser transitions. We have also found some unknown laser transitions in Ni-like tantalum and the optimum plasma parameters for laser action on these transitions.

1. INTRODUCTION

There are three steps for laser modeling in a plasma:

- Magneto hydrodynamic (MHD) calculations of plasma heating and plasma dynamics,
- Atomic-kinetic calculations of level populations and gain values.
- Calculations of light propagation in the plasma with an estimate of the saturation and coherence lengths.

Every step is a complicated problem that is dependent on many parameters. Since plasmas exhibit laser gain at a definite range of plasma parameters it is reasonable to produce preliminary atomic-kinetic calculations of gain values to establish the optimum plasma parameters for laser action on every possible transition. In these calculations we assume that to a first approximation MHD and atomic-kinetics are independent problems because level excitation by electrons have little influence on plasma gas dynamics.

Our earlier calculations of line intensities and gain values[1-2] indicate that laser action in the soft x-ray region is possible on the innershell 2s-2p transitions of Ne-like ions. Atomic-kinetic calculations were made for Ne-like krypton at 5.02 nm[2]. Later this effect was investigated in more detail for Ne-like germanium and yttrium[3]. In this work shortwavelength laser gain was predicted on collisionally pumped highly excited 2s hole states of Ne-like ions in preformed plasma. In recent works[4-5] it was found that laser gain is also possible on the transitions between highly excited states of Ne-like ions. In the cited works we searched for the optimum plasma parameters for laser gain. It was found that collisional line broadening of laser transitions is much larger than Doppler broadening. If collisional level mixing dominates then the upper and lower active level populations are of the same order in magnitude. Typically a laser inversion for level populations $P_u - P_l(g_u/g_l)$ is less than 10% of the upper level population. In Figure 1 patterns for level populations behavior as a function of electron density are presented for Ne-like silver at an electron temperature of T_e=3 keV. For most transitions in Ne-like silver the largest gain is possible at electron density $n_e \sim (2\text{-}5)\times10^{22}$ cm^{-3}. In such a dense plasma the level populations must be calculated with as high accuracy as possible. Thus the high accuracy atomic data and associated gain values together with their tendencies along the sequence are the key to x-ray laser development. This paper summarizes the previous investigations[1-5]. The results are given along the Ne-like sequence, so that the regularities can be seen for x-ray laser modeling along Z – Z is nuclear charge.

Part of the SPIE Conference on Soft X-Ray Lasers and Applications III • Denver, Colorado • July 1999
SPIE Vol. 3776 • 0277-786X/99/$10.00

Downloaded From: http://proceedings.spiedigitallibrary.org/ on 03/27/2014 Terms of Use: http://spiedl.org/terms

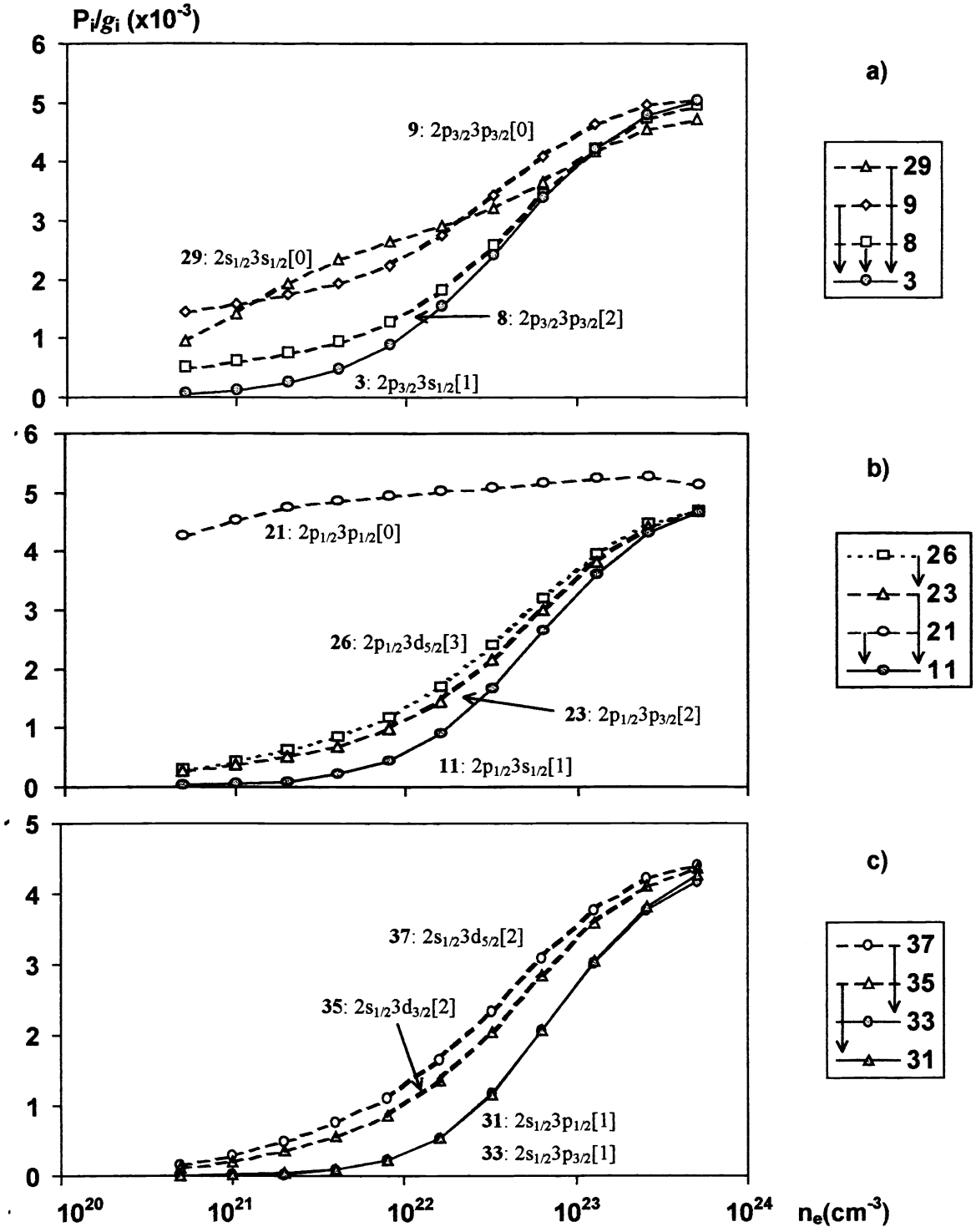


Fig 1. Populations (divided by statistic weights) of the upper and low active levels of Ne-like silver vs plasma electron density at T_e=3 keV. Plasma diameter is assumed to decrease with density (see text for more explanations).

Downloaded From: http://proceedings.spiedigitallibrary.org/ on 03/27/2014 Terms of Use: http://spiedl.org/terms

2. ATOMIC-KINETIC CALCULATIONS WITH APPLICATIONS TO X-RAY LASER MODELING

The calculations of energy levels, radiative transition probabilities (RTP) and electron collision strengths (ESC) are based on the uniform energy approach of quantum electrodynamics (QED). This method for atomic data calculations is known as relativistic perturbation theory with model potential (RPTMP). It is described elsewhere [6-10].

Atomic data calculations along the Ne-like sequence indicate that the optimum plasma electron density and the optimum ion density for laser action increases with Z. This conclusion follows from consideration of figures 2-4. Figure 2 shows that RTP from low active levels to the ground state grow along Z. The RTP for three laser transitions along Z are shown in figure 3 The rate of growth is different for each of the resonant transitions of figure.2, and some transitions irregularities are possible as functions of Z. The rate of radiative depletion of the low active level $2p_{1/2}3s_{1/2}[J=1]$ reaches the extreme value $2.x10^{14}$ s^{-1} at Z=53,54. This result is confirmed by other theories[6]. It was found[6] that level ordering can change at certain atomic numbers—they interact strongly at certain Z values. It is often associated with a vanishing oscillator strength in one radiative channel and an enhancement of the radiative strength in a competing channel. Thus RTP can be extremely sensitive to small changes in the model potential. This sensitivity is often due to strong cancellation of one-particle electron and one-particle inner-shell hole contributions and to two-particle contributions to correlation and relativistic effects. Higher order corrections of the perturbation theory become important as a result of such cancellations. These corrections are especially pronounced in the Ne-like and Ni-like sequences, as are configuration interaction effects. In the case of strong level interaction line intensities may be extremely sensitive to external plasma microfields. The effects of plasma microfields on the spectra of Ne-like and Ni-like ions were discussed recently[10].

In figure 4 the collisional level widths $\Delta\nu_i$ are shown along the Ne-like sequence calculated at impact electron energy equal to the ionization energy of the Ne-like ion: $\Delta\nu_i = \sum R_{ij}$ (cm^{-3},s^{-1}), where R_{ij} is the rate coefficient of the collisional transition from the i-th to the j-th level. The electron collisional mixing responsible for line width formation decreases along the sequence. Thus figures 2-4 indicate that electron and ion densities and gain values increase with Z. Ionization balance and lifetime of the Ne-like stage in the plasma are important factors which control the gain values. In gain calculations for each element the range of plasma electron temperature corresponds to the Ne-like stage. Also, the enhancement on the transitions of Ni-like tantalum is considered. The plasma is assumed to be uniform and stationary. In this case the plasma state is described by 5 parameters—electron and ion densities (n_e, n_i), temperatures (T_e,T_i) and plasma thickness, d. The free electron and ion distributions are taken to be Maxwellian. For level population calculations we use the approach [11] suitable for plasmas containing two kinds of ions of the adjacent ionization stage. In the balance equations for level populations 37 states of Ne-like ions are accounted for, i.e. the states of the configurations $2s^22p^5nl$, $2s2p^6nl$ $(n=3,\ l=0\text{-}2)$. This is the "basic" calculation accounting for six low configurations. In point 3 for Ne-like silver we investigate the convergence of the final results over the number of states in the kinetics. In the balance equations the states and radiative-collisional transitions between them are accounted for explicitly for Ne-like ions, while those for the infinite number of autoionizing Rydberg states of adjacent Na-like ions are accounted for by 37 energy zones. The population distribution of each zone is described by a continuous function of energy. This allows the inclusion in the kinetics of a diffusion-like motion of excitation over energy zones. For a more accurate kinetic description each adjacent zone is subdivided into three energy zones giving the total number of balance equations of 37+3x37=148.

In the plasma the principal elementary processes connecting two ionization stages—dielectronic capture by Ne-like ions, autoionization decay of Na-like ions, impact ionization of Na-like ions, triple recombination on Ne-like ions, electron impact and spontaneous radiative transitions between Rydberg zones and photorecombination—are accounted for by simple semi-classical formulae. The radiation reabsorption in a long plasma cylinder is included[12] through the escape factor. We obtain the level population values by integrating the balance equations with definite initial conditions.

The possibility of observing laser radiation is determined by proper plasma parameters n_e,T_e, d as well as by the abundance of the Ne-like stage and its lifetime in the plasma. Lifetime is a key factor. In a plasma dominated by a collisional-radiative mechanism it is determined by the time-scale of the Ne-like stage ionization to the next F-like stage. The radiative and other cooling mechanisms are less important. The result of integration is an estimate of the timescale of the Na-like ionization stage transformation to the Ne-like stage as a function of plasma conditions and the ratio of T_e/E_{ioniz} , E_{ioniz}(Na) is the ionization potential of the Na-like ion. Thus, time-scale estimates are possible for the Ne-like stage ionization to the next F-like stage. The lifetime of the Ne-like stage depends strongly on n_e. The dependence on T_e is less pronounced if $0.2\times E_{ioniz}<T_e<E_{ioniz}$ (E_{ioniz} is the ionization potential of the Ne-like ion.). The rates of elementary processes in plasmas involving electrons and multicharged

Downloaded From: http://proceedings.spiedigitallibrary.org/ on 03/27/2014 Terms of Use: http://spiedl.org/terms

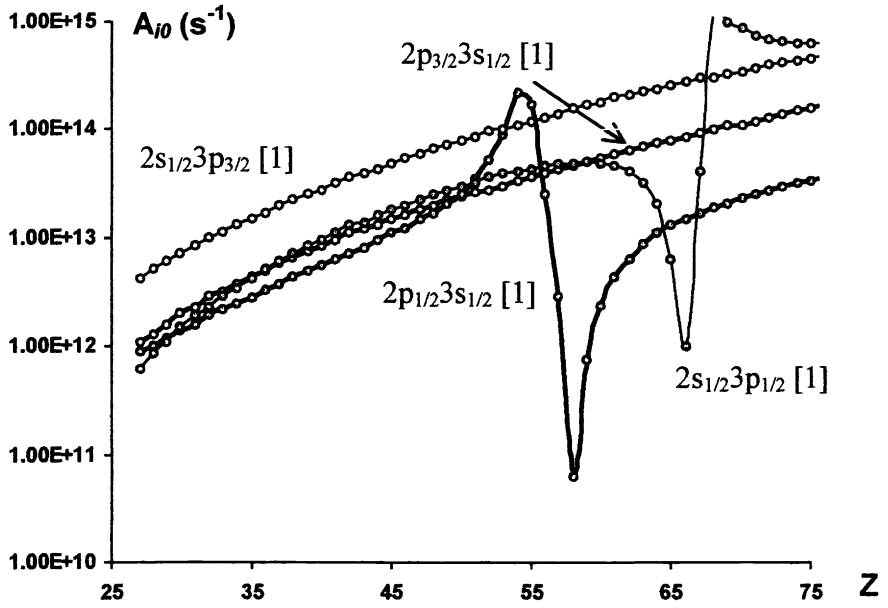


Fig 2. Rates for radiative depletion of low active levels along the Ne-like sequence.

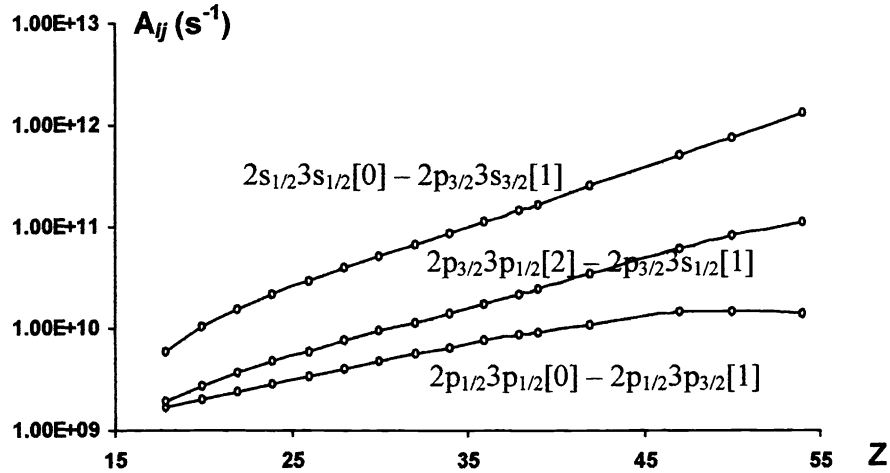


Fig 3. Radiative transition probability from upper to lower active level along the Ne-like sequence

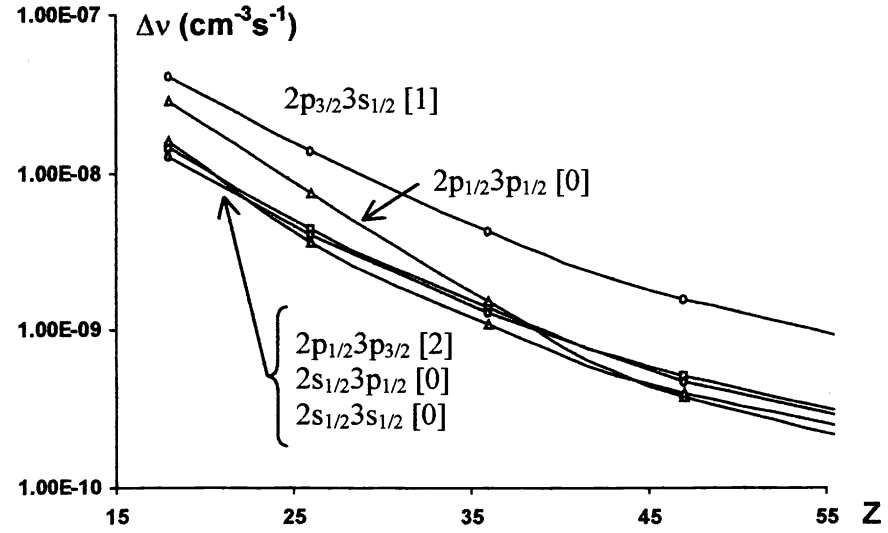


Fig 4. Collisional level widths along the Ne-like sequence calculated at impact electron energy $E_{imp} = E_{ioniz}$ (E_{ioniz} is the ionization energy of Ne-like ion)

Downloaded From: http://proceedings.spiedigitallibrary.org/ on 03/27/2014 Terms of Use: http://spiedl.org/terms

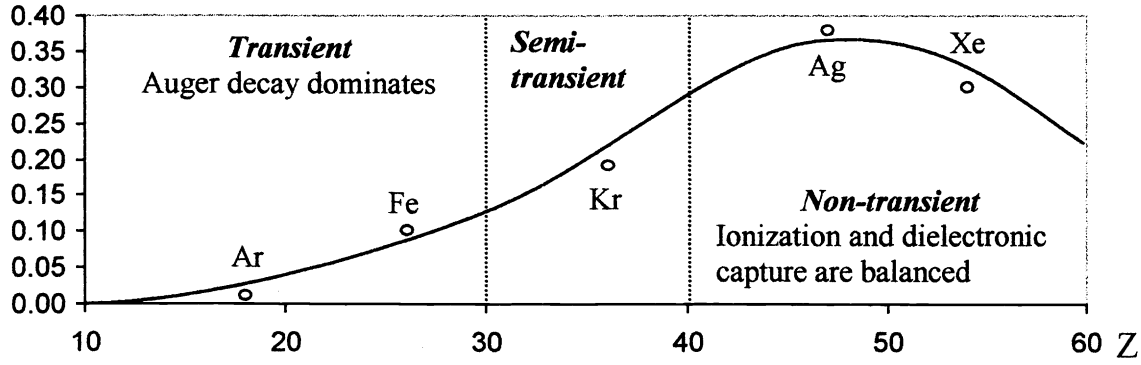


Fig.5. Fraction of Ne-like ions along the sequence in a steady state plasma at $T_e=E_{ioniz}/2$, and optimum n_e

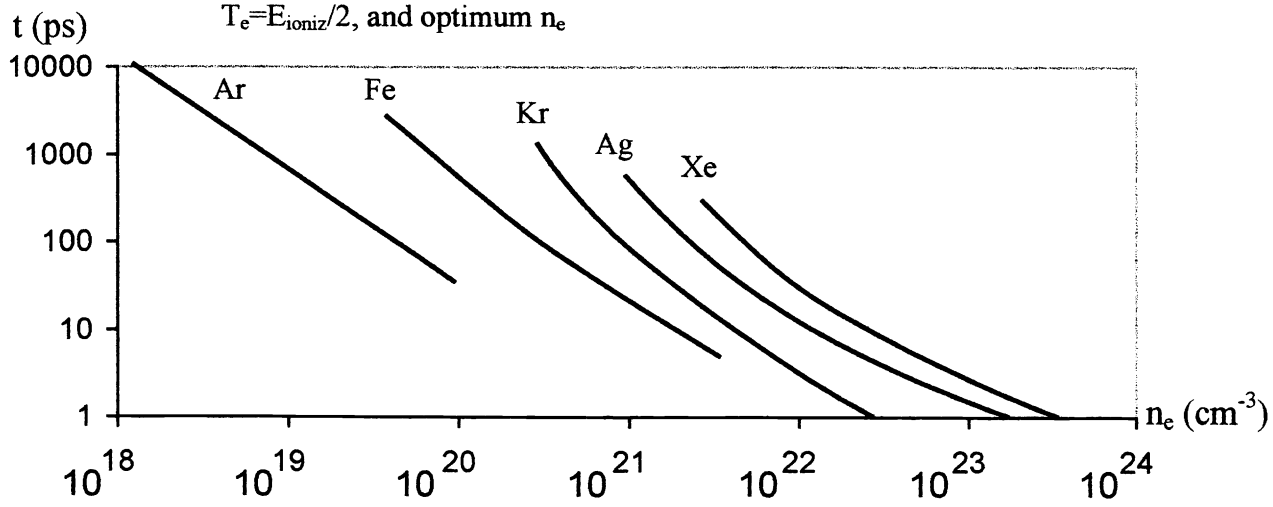


Fig.6. Time of Ne-like stage transformation to F-like at $T_e=E_{ioniz}/2$, as function of n_e

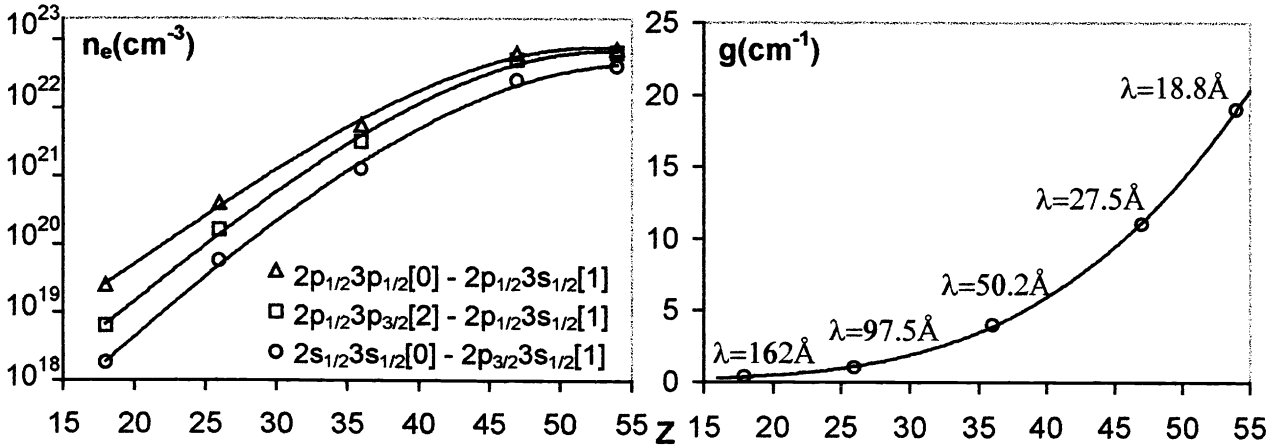


Fig. 7. Optimum n_e for lasing at $T_e=E_{ioniz}/2$ along the Ne-like sequence

Fig. 8. Gain on the 2s-2p innershell transition of Ne-like Ar, Fe, Kr, Ag and Xe, calculated at optimum n_e, $T_e=E_{ioniz}/2$, d=100 μm

Downloaded From: http://proceedings.spiedigitallibrary.org/ on 03/27/2014 Terms of Use: http://spiedl.org/terms

ions depend strongly on the ion charges. Thus Ne-like abundance in a steady-state plasma depends on the ion charge. There are three regions along the Ne-like sequence—they are shown approximately on figure 5. For each element we consider a plasma at $T_e = E_{ioniz}/2$ and the optimum electron density n_e^{opt}.

I) Low Z elements (Z<30) Auger decay and electron impact ionization dominates over dielectronic capture. Thus the Ne-like stage overionizes rapidly to the next F-like stage. Thus a steady-state plasma as $t \to \infty$ gives a Ne-like stage abundance that is very small: ~1% in an argon plasma and ~9% in an iron plasma.

11) For a plasma of moderate Z (30<Z<40) ionization processes still dominate over dielectronic capture; however as $t \to \infty$ (12-20%) of all ions remain in Ne-like stage.

III) The region of high Z (Z>40) corresponds to the balance of ionization and dielectronic capture processes.

In figure 6 we treat the variation along the sequence for the time for Ne-like stage transformation to F-like stage. For each element the time of transformation is shown as dependent of n_e—for each element $T_e = E_{ioniz}/2$. In figure 7 n_e^{opt} is shown for two ordinary transitions: 2p3p[J=0] - 2p3s [J=1] , 2p3p [J=2] – 2p3s [J=1] and for the innershell transition 2s3s [J=0] – 2p3s [J=1]. For low Z elements n_e^{opt} is the largest for the 0-1 (3p-3s) transition, while n_e^{opt} for the 2-1 (3p-3s) transition is about three times smaller. For elements with Z>45, n_e^{opt} for both transitions is practically the same. For the 0-1 (2s-2p) transition n_e^{opt} is the smallest. The gain values for the innershell transition of Ne-like Ar, Fe, Kr, Ag and Xe, calculated at n_e^{opt} , $T_e=E_{ioniz}/2$, d=100μm are plotted in figure 8. The gain will reach its maximum value and will diminish in the limit of large Z (Z>60) where Doppler broadening dominates.

The gains for other transitions at optimum n_e, T_e, and d also grow along the Ne-like sequence. Optimum gain for the 2-1 (3p-3s) transition is larger than that for the 0-1 (3p-3s) transition. We found that laser action is possible on the transitions between highly excited states. The largest gains correspond to the two 2-1 (2s3d-2s3p) transitions. 2s3d is the highest configuration accounted for in the kinetics for 37 levels. The level populations for this configuration depend on the inclusion of the higher configurations $2s^22p^54l$, $2s2p^64l$ into the set of balance equations.

3. CONVERGENCE OF FINAL RESULTS OVER THE NUMBER OF STATES IN THE BALANCE EQUATIONS.

We investigated the convergence of gain calculations over the number of states in the kinetics for Ne-like silver. This element was chosen as a possible material for production of a large ASE effect using a short pulse, high power laser as a pump source[4]. In cited work a list of promising laser transitions in the Ne-like silver is presented. Most of them were never investigated or mentioned earlier. The gain calculations[4] were made by accounting for only 37 levels of configurations $2s^22p^5nl$, $2s2p^6nl$ ($n=3$, $l=0-2$). Here we do similar calculations by accounting for additional states with $n=4$, $l=0-3$. Thus the total number of balance equations in the kinetics is 89+ 89×3=356. Figures 9a,b demonstrate the comparison of the two approximations for gain calculations in Ne-like silver—basic calculations (solid lines) obtained by accounting for 37 levels and extended calculations (dashed lines) obtained by accounting for 89 levels. Gain dependence on n_e is given for T_e=2 keV (circles) and T_e=4 keV (triangles). For transitions between the low excited levels $n_e^{opt} = (3\text{-}5) \times 10^{22}$ cm^{-3} and the gain values were practically the same in both approximations. The gain value at $n_e^{opt} = (2\text{-}5)\times 10^{22}$ cm^{-3} for the 0-1 (2s-2p) innershell transition in the extended calculation was about 20% larger than in the basic calculation.

Figure 9b demonstrates the convergence of calculations for newly found transitions between highly excited states. The results for both the 2-1 (2s3d-2s3p) transitions are stable within an accuracy of 20-25%. For these transitions the inversion population is due to very fast depletion of 2s3p [J=1] states—the large gain at relatively low temperature is conditioned by rapid population of the upper active levels 2s3d [J=2] from the ground state and by large RTP from the upper to low active level.

Our calculations show that another mechanism of inversion is possible in the collisional-radiative model. For example we discuss the transition $2p_{1/2}3d_{5/2}$ [J=3] – $2p_{1/2}3p_{3/2}$ [J=2].. Here the inversion arises due to slow depopulation of the upper level with J=3. The low level with J=2 is depopulated faster. At the same time this level with J=2 is inverted relative to the 2p3s [J=1] level. The stability of the gain calculation for the 3-2 (3d-3p) transition was within 50%.

Downloaded From: http://proceedings.spiedigitallibrary.org/ on 03/27/2014 Terms of Use: http://spiedl.org/terms

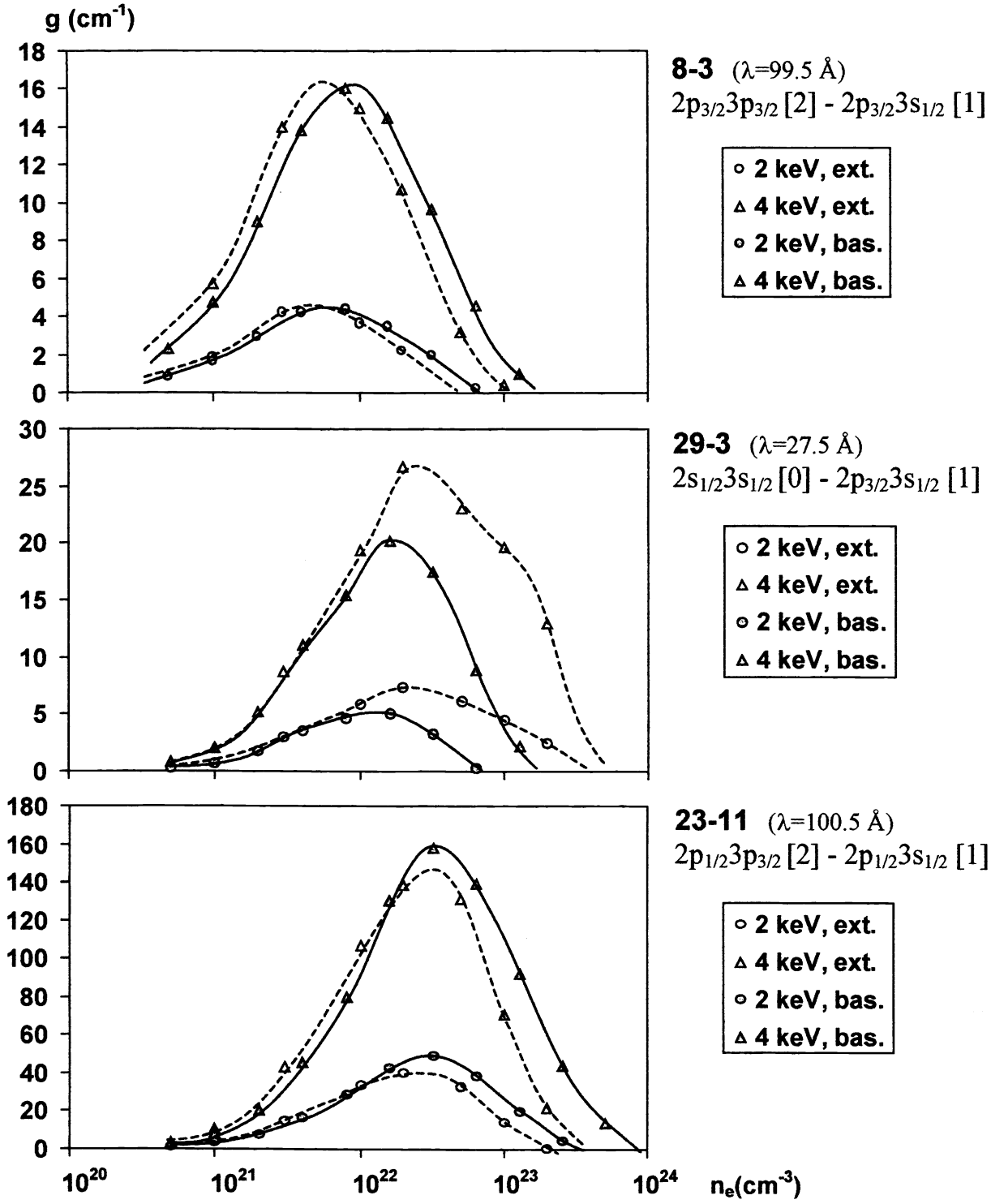


Fig 9a. Comparison of two approximations for gain calculations in Ne-like silver: "bas" (solid lines) shows basic calculation which accounts for 37 levels; "ext" (dashed line) shows extended calculation which accounts for 89 levels. Gain dependence on n_e is given for two values of T_e : circles for T_e=2 keV triangles for T_e= 4 keV .

Downloaded From: http://proceedings.spiedigitallibrary.org/ on 03/27/2014 Terms of Use: http://spiedl.org/terms

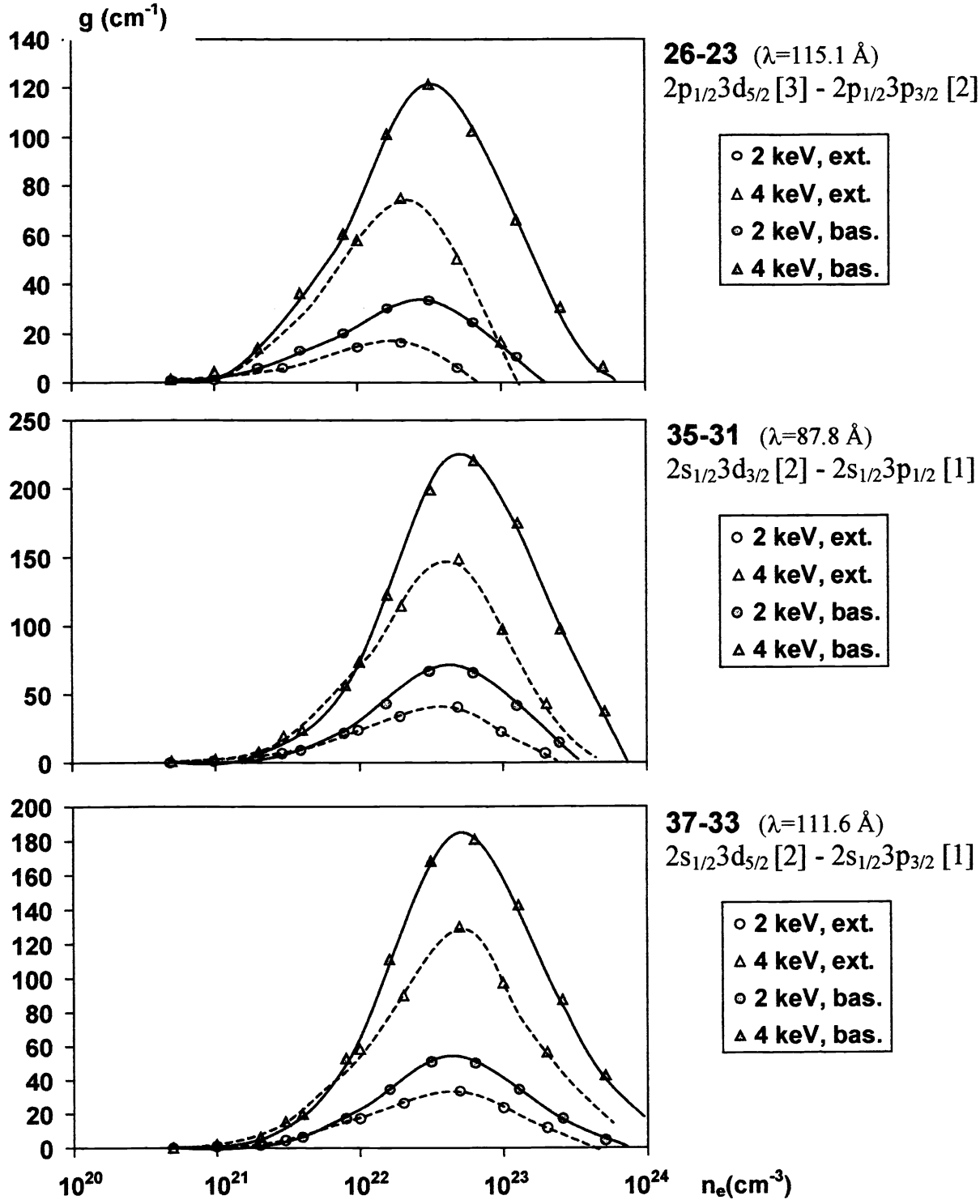


Fig 9b. Comparison of two approximations for gain calculations in Ne-like silver for transitions between highly excited states: "bas" (solid line) shows basic calculation which accounts for 37 levels; "ext" (dashed line) shows extended calculation which accounts for 89 levels. Gain dependence on n_e is given for two values of T_e : circles for T_e=2 keV triangles for T_e= 4 keV .

Downloaded From: http://proceedings.spiedigitallibrary.org/ on 03/27/2014 Terms of Use: http://spiedl.org/terms

In summary we state that most gain calculations are in principle stable over the number of levels in the kinetics. Thus, for all other ions we use the simple basic model which accounts for 37 Ne-like states.

4. GAIN CALCULATIONS FOR Ne-LIKE ARGON, IRON, KRYPTON, SILVER, AND XENON

We have made calculations of gain for Ne-like argon in the plasma of a capillary discharge for each possible laser transition. The gain dependence on plasma parameters, n_e, T_e and d are evaluated. In figure 10a the dependence is given for the 0-1, 2-1 (3p-3s) laser transitions with lower active level $2p^5 3s$ [J=1]. This figure shows that laser action can occur on the 0-1 (3p-3s) laser transition at λ=469 Å at a much larger n_e than for the 2-1 (3p-3s) transition at λ=698 Å. A theoretical estimate of the temporal parameters and their comparison with experimental data [13-15] make it possible to determine the plasma parameters for these experiments[16]. Laser action on the innershell 0-1 (2s-2p) transition is possible with a gain 0.2 – 0.4 cm^{-1} if $n_e \sim (2\text{-}7)\times10^{18}$ cm^{-3}, $T_e \sim$ 200-300 eV, and d≤200 μm. We found that the largest gain occurs at the 2-1 (2s3d-2s3p) transition at λ=520 Å. This led to the surprising conclusion that laser action on this transition is possible at moderate and low T_e.

The dependence of gain on n_e, T_e in plasmas of 100 μm width for selected transitions of the Ne-like iron is presented on figure 10b. For the 0-1 (3p-3s) transition, $n_e = 10^{20} - 3\times10^{21}$ cm^{-3} if T_e = 150 – 1000 eV. At Te=1 keV gain g = 12-15 cm^{-1}. The maximum density for the 2-1 (3p-3s) transition is $n_e = 5\times10^{20}$ cm^{-3} . The maximum possible gain is about 40 cm^{-1} at $n_e^{opt} = 2\times10^{20} cm^{-3}$. The maximum possible gain for the innershell 0-1 (2s-2p) transition is 1-2 cm^{-1} if Te>500 eV and $n_e^{opt}=10^{20}$ cm^{-3}. Also are shown n_e,T_e dependencies for a new type transition between highly excited states – 2-1 (2s3d-2s3p) transitions and 2-1 (2s3p-2s3s).

A Ne-like laser for low Z-elements was demonstrated, where the 0-1 (3p-3s) transition is the dominant laser transition using a prepulse technique. The first observation of transition enhancement was made for Ne-like titanium[17]. Later a prepulse technique was used to obtain 0-1, 2-1 (3p-3s) lasers for Ne-like iron, chromium and titanium[18]. For all ions the strongest laser action was observed at the 0-1 (3p-3s) transition. ASE for the 2-1 (3p-3s) transition was weaker. In a recent work[19] laser action on the 0-1 (3p-3s) transition was investigated in more details to find the pump laser configuration for achieving the highest gain on two successive pulses. The maximum gain was 15 cm^{-1} with a gain length product as large as 25.

Earlier attempts to produce laser action using a single long-lasting pump pulse (0.5-1 ns) for low-Z elements (Z<29) were not successful. The problem was that the plasma density region – close to n_e^{opt} – was nonuniform in a single pump experiments. A prepulse technique improved the plasma uniformity. However plasma density in these experiments corresponded to the maximum n_e for lasing on the 0-1 (3p-3s) transition. At this n_e laser action on the 2-1 (3p-3s) transition is less pronounced, and the 0-1 (2s-2p) transition does not generate laser action.

Figure 10c shows the gain dependence on n_e, T_e for selected transitions of Ne-like krypton. The atomic data for this ion are similar to those of ions in the range 32<Z<40. The rates for RTP, ESC, $\Delta\nu_I$ are more favorable for lasing on the transitions of these moderate Z ions. Thus the number of candidates—transitions showing laser action—increases for this Z-region. On the other hand the laser effect is not absolutely transient because some of the ions remain in the Ne-like stage at steady-state plasma conditions. In this case n_e^{opt} is in the range 7×10^{20} - 5×10^{21} cm^{-3} depending on the transition and T_e. In the first experiments[20-21] with a single pump pulse the n_e for the quasi-uniform part of plasma was less than 10^{21} cm^{-3}. Thus at relatively small T_e both 2-1 (3p-3s) transitions produced a stronger effect than the 0-1 (3p-3s) transitions. In Ne-like krypton the laser action on the 0-1 (2s-2p) transition is noticeable at T_e=600-700 eV if $n_e=10^{21}$ cm^{-3}. The gain value grows fast with T_e. Thus g~ 5-6 cm^{-1} at $T_e=E_{ioniz}/2$. We believe that at this value of T_e laser action below water window—at λ=42 Å—is possible in a plasma of the Ne-like yttrium

The gain values of selected transitions of Ne-like silver are given in figure 10d. These are results are from extended calculations which account for 89 levels in the kinetics for Ne-like ion.. The plasma width is assumed to decrease with n_e from d=100 μm at $n_e=10^{21}$ cm^{-3} to d=5 μm at $n_e=10^{23}$ cm^{-3}. Laser action with gL>100 on the transitions of this element is discussed in detail in our earlier works[4,22] and elsewhere in this paper.

Gain coefficients as functions of n_e, T_e for selected transitions of Ne-like xenon for plasmas of 100 μm width are given in figure 10e. Figure 2 shows that there is a very fast depletion channel for the lower active level $2p_{1/2}3s_{1/2}$ [J=1] for Z=53,54. Thus we expected the increase of the inversion and gain values for the transition to this level. The calculations for gain have shown that the number of possible laser transitions in Ne-like xenon is larger that in Ne-like silver. Most transitions can lase at T_e=2keV if $n_e=10^{22}$ cm^{-3} with gain values of few cm^{-1}. For larger T_e laser action is possible at $n_e=(3\text{-}5)\times10^{22}$ cm^{-3} with much larger gain values. The giant gain is predicted for the 2-1 (2s3d-2s3p) transition at 61.6 Å if T_e≥3 keV. Å

Downloaded From: http://proceedings.spiedigitallibrary.org/ on 03/27/2014 Terms of Use: http://spiedl.org/terms

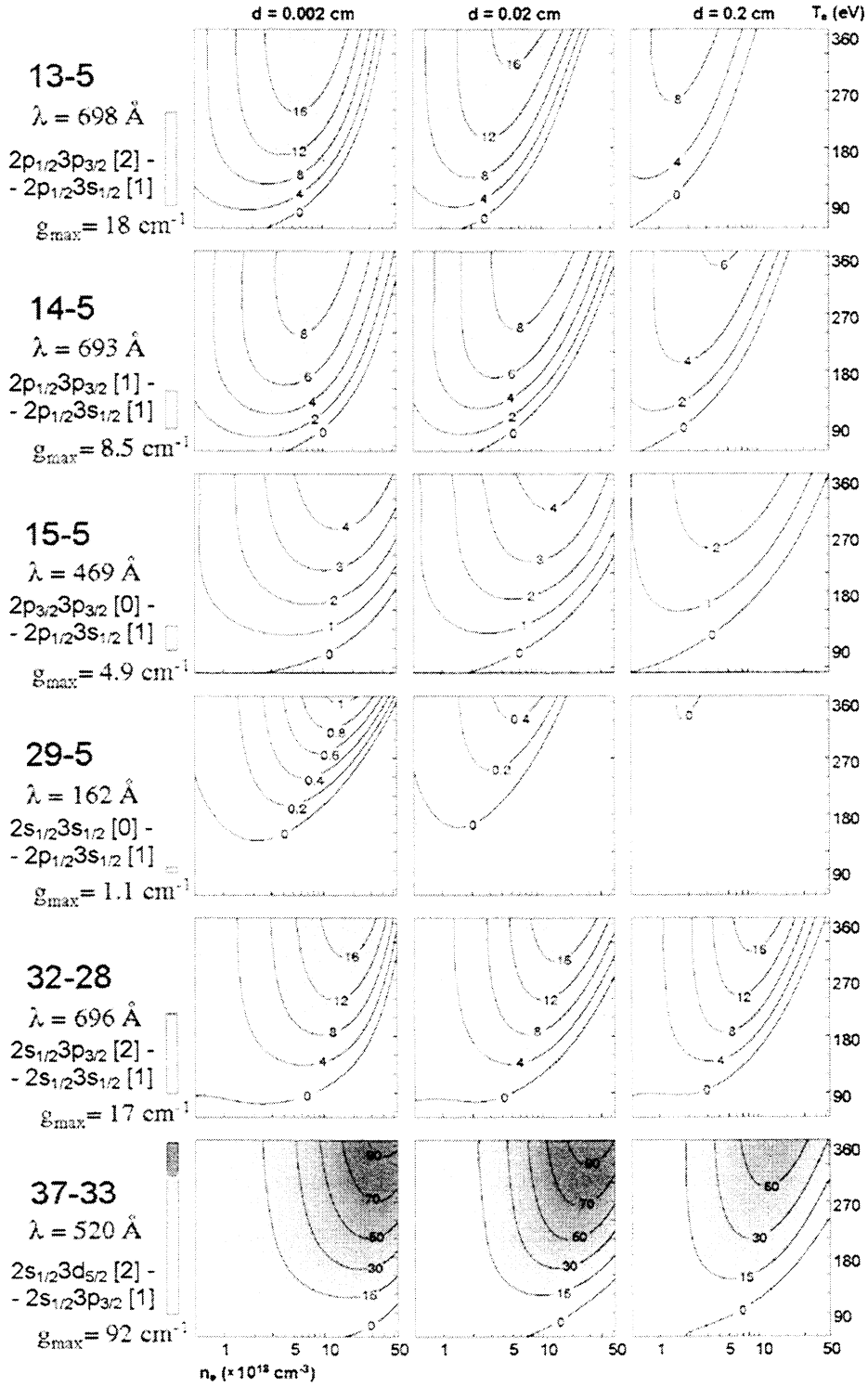


Fig. 10(a). Gain coefficients as functions of n_e (cm^{-3}), T_e (eV) for selected transitions of Ne-like argon (Z=18) for steady-state uniform plasma at different plasma diameter d.
a) d=0.002 cm
b) d=0.02 cm
c) d=0.2 cm

Downloaded From: http://proceedings.spiedigitallibrary.org/ on 03/27/2014 Terms of Use: http://spiedl.org/terms

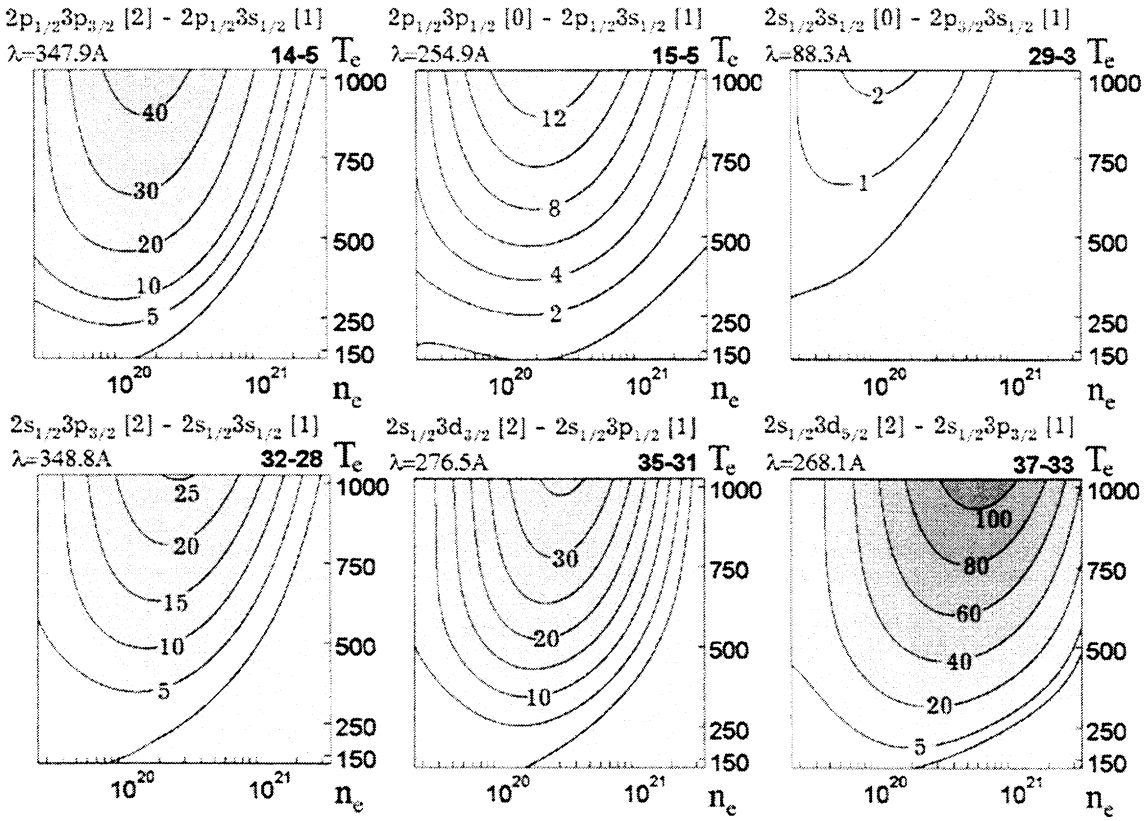


Fig. 10(b). Gain coefficients as functions of $\mathbf{n_e}$ **(cm^{-3})**, $\mathbf{T_e}$ **(eV)** for selected transitions of Ne-like iron **(Z=26)** for steady state uniform plasma **200μm** width.

Downloaded From: http://proceedings.spiedigitallibrary.org/ on 03/27/2014 Terms of Use: http://spiedl.org/terms

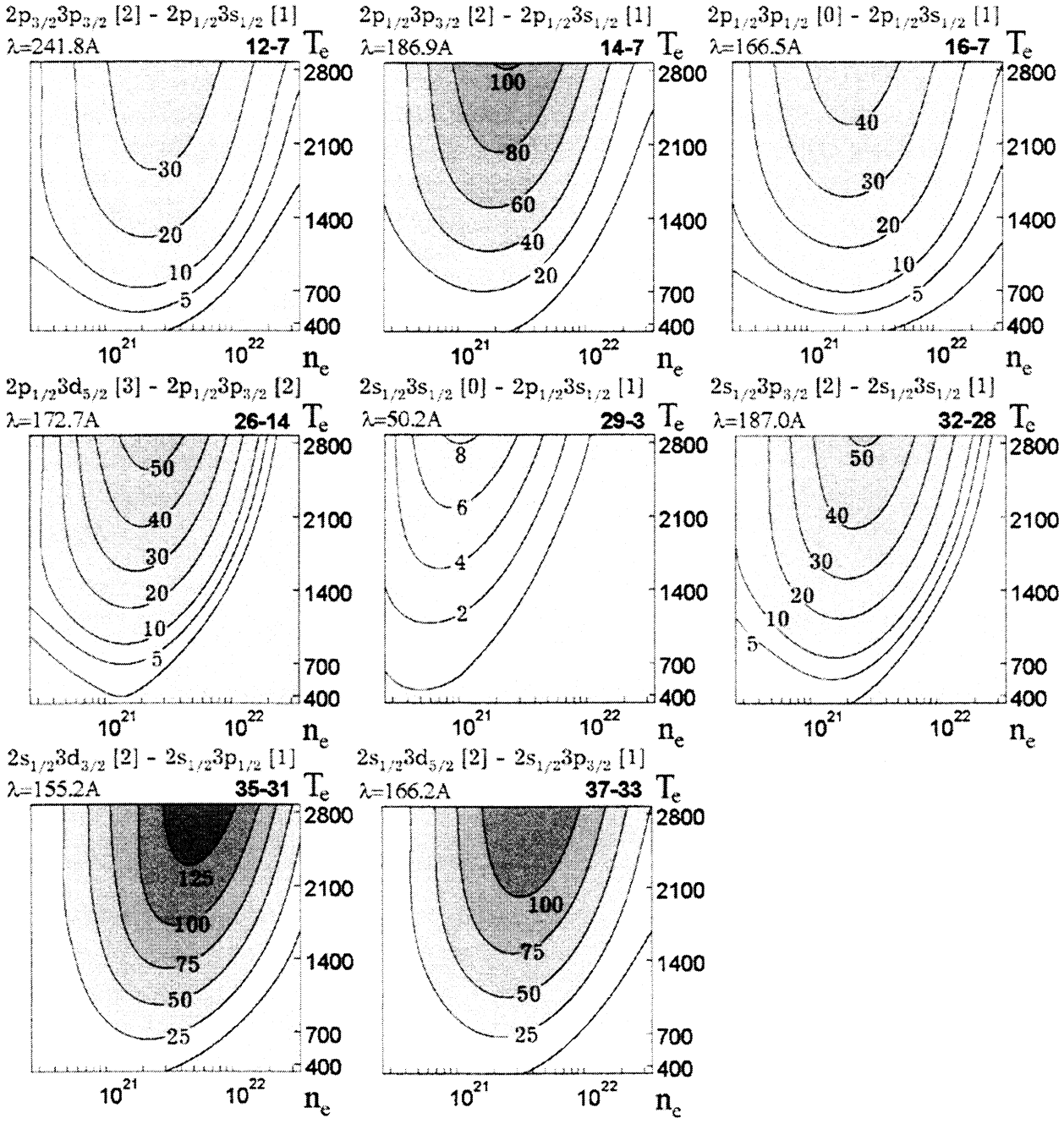


Fig. 10(c). Gain coefficients as functions of n_e **(cm^{-3})**, T_e **(eV)** for selected transitions of Ne-like krypton **(Z=36)** for steady state uniform plasma **200μm** width.

Downloaded From: http://proceedings.spiedigitallibrary.org/ on 03/27/2014 Terms of Use: http://spiedl.org/terms

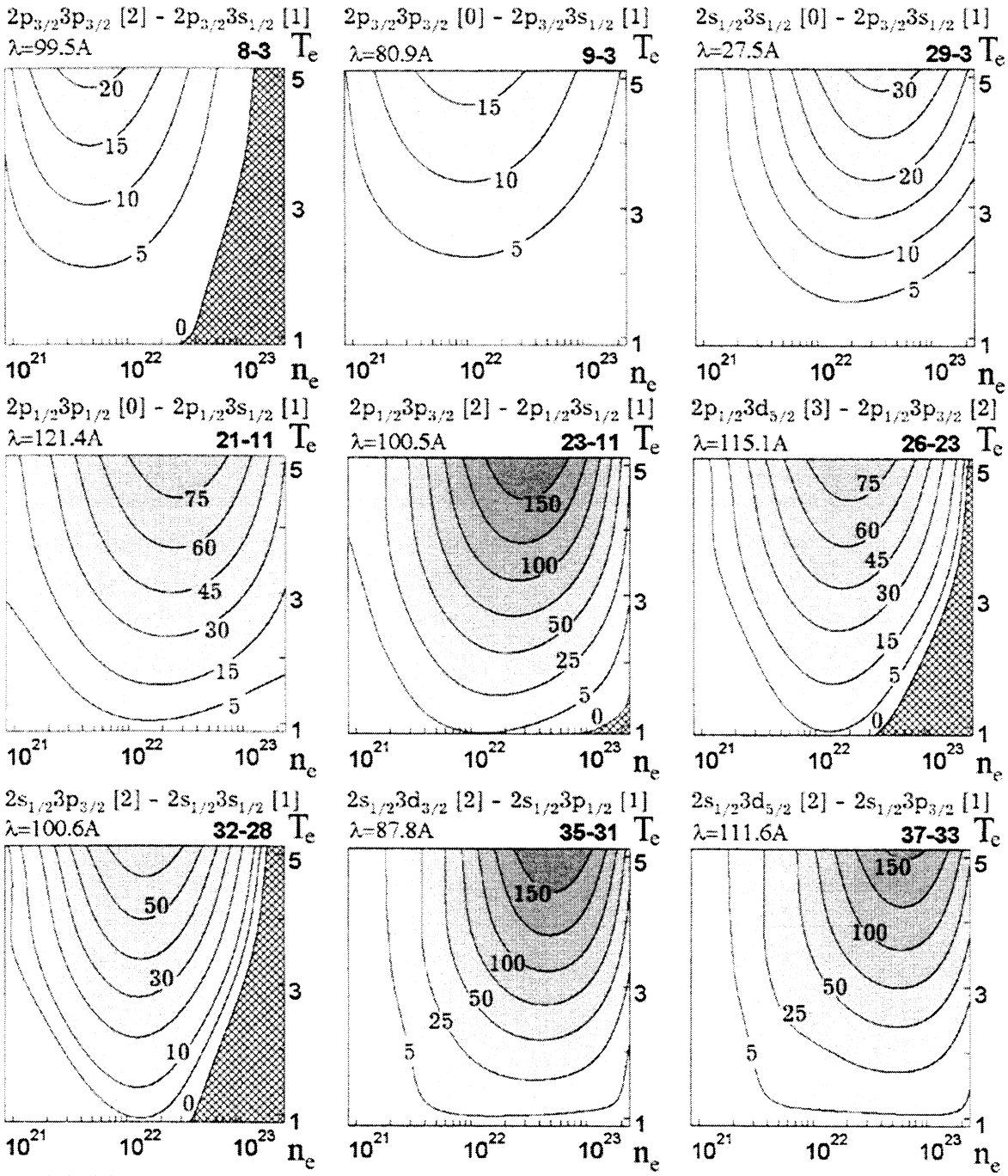


Fig. 10(d). Results for extended calculations of gain values as functions of n_e **(cm^{-3})**, T_e **(keV)** for selected transitions of Ne-like silver **(Z=47)**. Plasma diameter assumed to decrease with n_e from **d**=100μm at $n_e=10^{21}$cm^{-3} to **d**=5μm at $n_e=10^{23}$cm^{-3}.

Downloaded From: http://proceedings.spiedigitallibrary.org/ on 03/27/2014 Terms of Use: http://spiedl.org/terms

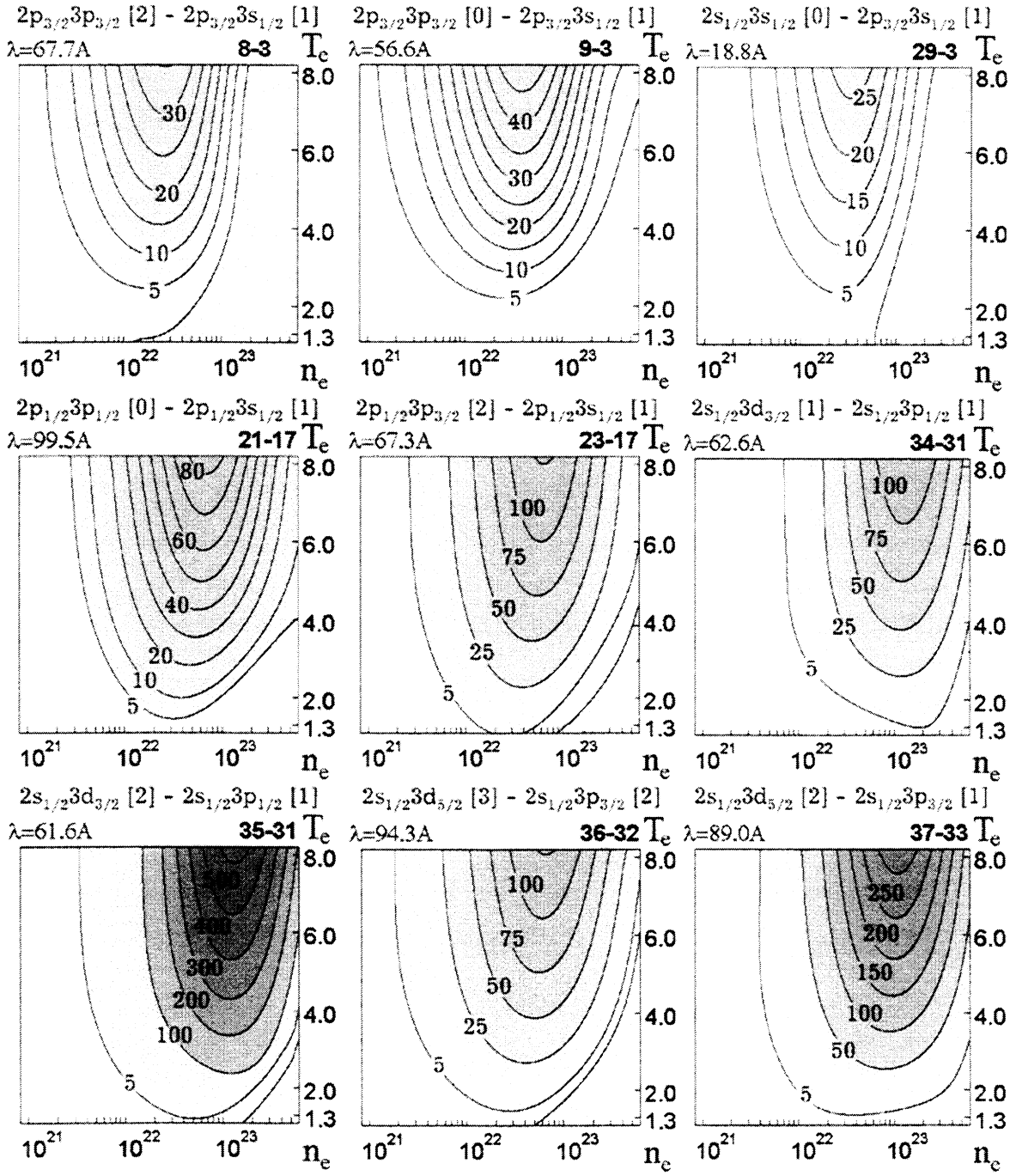


Fig. 10(e). Gain coefficients as functions of n_e **(cm^{-3})**, T_e **(keV)** for selected transitions of Ne-like xenon **(Z=54)** for steady state uniform plasma **100μm** width.

Downloaded From: http://proceedings.spiedigitallibrary.org/ on 03/27/2014 Terms of Use: http://spiedl.org/terms

5. GAIN CALCULATIONS FOR THE Ni-LIKE TANTALUM X-RAY LASER

Intense research is currently being carried out to demonstrate ASE for the Ni-like ion scheme operating at saturation[23-25]. Here we continue the investigations initiated during last decade[26-31]. In a recent work[10] the large disagreement between *ab initio* theoretical and experimental wavelengths for the 0-1 (4d-4p) laser transition along the Ni-like sequence was analyzed. This anomaly can be attributed to plasma electric microfield influence on the position of highly excited even levels with J=0. Their positions are the result of cancellations of correlation contributions as they interact strongly. Thus a small disturbance of the atomic orbital by an external field can lead to a noticeable change in state energies.

Here we present results for gain calculations on the transitions of Ni-like tantalum in a uniform plasma of 100 μm width. The promising transitions for laser action are listed in Table 1. For these transitions wavelengths, RTP from upper to lower levels are given. Rates of electron collisional excitation from the ground state (R_{ECEG}) for upper active levels are also given. They are calculated at T_e=1.5 keV. For each transition the gain is estimated for the set of plasma parameters. Enhancement is possible at the water window wavelength—44 Å—at $n_e^{opt} = 1.5\times10^{21}cm^{-3}$ – the gain dependence on T_e for different n_e is given in the Table 1. We found that laser action is possible between highly excited states of Ni-like tantalum. Thus new types of transitions are found. The largest gain for Ni-like tantalum occurs at the 4-3 (4f-4d) transition at wavelengths 71.52 Å and 78.03 Å. This is a new mechanism for inversion analogous to that discussed for the Ne-like ions. The inversion for these transitions is conditioned by two factors: i) fast population of the upper active levels with J=4 by electron impact from the ground state—large ECS and R_{ECEG}, ii) by large RTP from the upper to low active level. In Table 1 there are also laser transitions generated by the ordinary mechanism for inversion— mainly due to fast depopulation of the low active level.

The laser action on the innershell 0-1 (3p-3d) transition at λ=27.0 Å is possible if $T_e\geq2$ keV and $n_e\approx10^{21}$ cm^{-3}. Tantalum in the Ni-like stage was chosen for modeling because of the possibility of obtaining laser action below the water window—λ=44 Å. We do not consider other elements of the Ni-like sequence. However looking at RTP, ECS and $\Delta\nu_i$ along the sequence indicates that the largest gain in Ni-like ions corresponds to medium Z. We believe that laser action below the water window can be obtained using the innershell 0-1 (3p-3d) transition of Ni-like ions with Z<60.

5. CONCLUSION

Laser action is possible on the innershell 2s-2p transitions of Ne-like ions. The wavelength of 2s-2p transition is 3-4 times smaller than the wavelength of the ordinary 3p-3s transition in the same ion. Gain on the 2s-2p transition is possible if $T_e\geq E_{ioniz}/2$, and gain grows rapidly with T_e. Laser action below the water window is possible on the innershell transitions of Ne-like yttrium if $T_e\geq1.5$ keV.

Plasma conditions for laser action were studied along the Ne-like sequence for argon, iron, krypton, silver and xenon. The optimum n_e increases along the sequence so that $n_e^{opt} \sim (2\text{-}5)\times10^{22}$ cm^{-3} at Z>45. For low Z elements at given T_e and d, n_e^{opt} is different for each transition: i) n_e^{opt} is the largest for the 0-1 3p-3s transition; ii) n_e^{opt} is the smallest for the 0-1 innershell 2s-2p transition; iii) n_e^{opt} for the 2-1 3p-3s transition is of intermediate value—it is 2-3 times smaller than that for the 0-1 3p-3s transition. For all three transitions the optimum gain grows with Z.

With assumption that $T_e = (0.2\text{-}1.0)\times E_{ioniz}$ for low Z elements (Z<30) gain is transient due to fast overionization to the F-like stage—for low Z ions, Auger decay and ionization dominate dielectronic capture. For 30<Z<40 the gain is semi-transient at optimum parameters because 10-15% of the ions remains in the Ne-like stage. For Z>40 the gain is non-transient because ionization and dielectronic capture are balanced.

New laser lines are predicted which correspond to transition between highly excited states. The most promising are two transitions—$2s_{1/2}2p^6 3d_{5/2}$ [J=2] – $2s_{1/2}2p^6 3p_{3/2}$ [J=1], and $2s_{1/2}2p^6 3d_{3/2}$ [J=2] – $2s_{1/2}2p^6 3p_{1/2}$ [J=1]. The stability for gain calculations over the number of states accounted for in the balance equations was shown.

On the basis of similar investigations for Ni-like tantalum, the plasma conditions for laser action on the innershell 0-1 (3p-3d) transition were found. Also the new laser transitions were found. The new laser transitions are subdivided into two groups: i) those created by the well known mechanism of inversion – fast radiative depopulation of lower active level;
ii) a new type of inversion due to very fast population by electron impact of the upper active level with a large RTP from upper to lower level.

Downloaded From: http://proceedings.spiedigitallibrary.org/ on 03/27/2014 Terms of Use: http://spiedl.org/terms

TABLE 1. Possible laser transitions in Ni-like tantalum., wavelengths and RTP from upper to the lower level,; rates of electron collisional excitation from the ground state (R_{ECEG}) for the upper levels are calculated at Te=1.5 keV. Gain values are estimated for steady state uniform plasma 100 μm width.

				GAIN (cm^{-1})								
				n_e=1.5×10^{21} cm^{-3}			n_e =3×10^{21} cm^{-3}			n_e=5×10^{21} cm^{-3}		
				T_e(keV)			T_e(keV)			T_e(keV)		
transition	λ(A)	RTP (s^{-1})	R_{ECEG} ($cm^{-3}s^{-1}$)	1.0	1.5	2.0	1.0	1.5	2.0	1.0	1.5	2.0
$2d_{5/2}4p_{1/2}$ [3]-$3d_{5/2}4s_{1/2}$ [2]	132.90	2.69+10	3.55-13	0.1	0.8	1.9	-	-	0.1	-	-	-
$3d_{5/2}4d_{3/2}$ [2]-$3d_{5/2}4p_{3/2}$ [1]	86.48	8.20+09	3.19-13	-	0.1	0.3	-	-	-	-	-	-
$3d_{5/2}4d_{5/2}$ [2]-$3d_{5/2}4p_{3/2}$ [1]	74.55	9.36+10	1.08-12	0.1	0.7	1.6	-	-	-	-	-	-
$3d_{3/2}4d_{3/2}$ [0]-$3d_{3/2}4p_{1/2}$ [1]	44.05	5.14+11	2.02-11	1.0	3.2	5.3	0.5	1.7	2.9	0.1	0.5	1.3
$3d_{3/2}4d_{3/2}$ [0]-$3d_{5/2}4p_{3/2}$ [1]	50.00	1.42+11	2.02-11	0.4	1.0	1.7	0.2	0.7	1.2	0.1	0.4	0.7
$3d_{3/2}4d_{3/2}$ [0]-$3d_{3/2}4p_{3/2}$ [1]	66.09	2.62+10	2.02-11	0.1	0.3	0.6	-	0.2	0.3	-	0.1	0.2
$3p_{3/2}4p_{1/2}$ [2]-$3p_{3/2}4s_{1/2}$ [1]	134.3	2.33+10	7.29-13	0.7	1.7	2.4	0.5	1.4	2.3	0.2	0.8	1.5
$3p_{3/2}4p_{3/2}$ [1]-$3p_{3/2}4s_{1/2}$ [1]	66.21	3.31+11	4.87-14	0.4	1.1	1.8	-	0.3	1.1	-	-	-
$3p_{3/2}4p_{3/2}$ [2]-$3p_{3/2}4s_{1/2}$ [1]	64.64	1.95+11	4.49-13	0.8	2.3	3.4	0.2	1.4	2.9	-	0.3	1.2
$3p_{3/2}4p_{3/2}$ [0]-$3d_{5/2}4p_{3/2}$ [1]	27.00	1.30+12	1.22-11	-	0.1	0.4	-	-	-	-	-	-
$3p_{3/2}4p_{3/2}$ [0]-$3p_{3/2}4s_{1/2}$ [1]	59.14	3.83+11	1.22-11	1.3	3.4	5.0	1.1	3.0	4.8	0.7	2.0	3.5
$3p_{1/2}4p_{1/2}$ [0]-$3p_{1/2}4s_{1/2}$ [1]	65.32	4.52+10	6.65-12	0.6	1.6	2.3	0.9	2.4	3.5	0.8	2.1	3.4
$3p_{1/2}4p_{3/2}$ [2]-$3p_{1/2}4s_{1/2}$ [1]	65.06	3.91+11	3.77-13	1.1	2.6	3.7	1.0	3.8	6.5	0.6	2.8	5.6
$3p_{3/2}4f_{5/2}$ [4]-$3p_{3/2}4d_{3/2}$ [3]	71.52	2.70+11	1.85-11	3.0	11.0	18.3	1.5	6.9	13.0	0.5	3.3	7.0
$3p_{3/2}4f_{7/2}$ [4]-$3p_{3/2}4d_{5/2}$ [3]	77.82	1.96+11	1.21-11	1.4	5.8	10.2	0.6	3.5	7.2	0.1	1.6	3.9
$3p_{3/2}4f_{7/2}$ [2]-$3p_{3/2}4d_{5/2}$ [1]	74.99	1.75+11	6.79-12	1.0	2.7	4.0	0.9	3.2	5.3	0.5	2.1	4.2
$3p_{1/2}4d_{5/2}$ [2]-$3p_{1/2}4p_{3/2}$ [1]	74.82	2.86+11	8.73-14	0.7	1.9	3.0	0.5	2.4	4.6	0.2	1.5	3.5
$3p_{1/2}4d_{5/2}$ [3]-$3p_{1/2}4p_{3/2}$ [2]	74.93	3.15+11	2.31-13	1.5	1.2	1.1	1.1	5.0	9.0	0.5	3.3	7.5
$3p_{1/2}4f_{7/2}$ [4]-$3p_{1/2}4d_{5/2}$ [3]	78.03	2.20+11	1.72-11	3.8	11.0	20.3	3.4	13.0	26.0	2.3	9.6	21.0

Downloaded From: http://proceedings.spiedigitallibrary.org/ on 03/27/2014 Terms of Use: http://spiedl.org/terms

REFERENCES

1. L. N. Ivanov, E. P. Ivanova, L. V. Knight, "Line intensities of Ne-like ions in plasma," Proceedings of SPIE"Ultrashort wavelength lasers II" edited by S.Suckewer, 10-12 July 1993, San-Diego, CA, Vol.2012, pp.265-272.
2. E. P. Ivanova, L. V. Knight and A. Reyes-Mena, "Plasma conditions for ASE observations from highly excited states of Ne-like Krypton", Proceedings of the International conference Lasers-94, 6-10 December, 1994, Quebec, Canada
3. S. B. Healy, K.A.Janulevicz, G.J.Pert, "Shortwavelength lasing on collisionally pumped, highly excited 2s hole states of neon-like ions in preformed plasma, irradiated with intense picosecond pulses", Opt. Commun., Vol.144, pp.24-30, 1997.
4. E. P. Ivanova, A. L. Ivanov, N. A. Zinov'ev and L. V. Knight, "Proposal for x-ray laser pumped by a powerful short-pulse-drive laser", Inst. Phys. Conf. Ser No 159. Paper presented at X-ray Laser Conf., Kyoto, 31 August – 4 September 1998, pp.399-402.
5. E. P. Ivanova and N. A. Zinov'ev, "Gain calculation in capillary discharge plasma", Inst. Phys. Conf. Ser No 159. Paper presented at X-ray Laser Conf., Kyoto, 31 August – 4 September 1998, p.199-202.
6. E. P. Ivanova and I. P. Grant, "Oscillator strength anomalies in the Ne-like isoelectronic sequence with application to x-ray laser modeling" J. Phys. B: At., Mol., Opt. Phys., Vol.31, pp.2871-2883, 1998.
7. E. P. Ivanova, L. N. Ivanov, A.E. Kramida and A. V. Glushkov, "High order corrections in the relativistic perturbation theory with the model zeroth approximation", Physica Scripta, Vol.32, pp. 513-522, 1985.
8. L. N. Ivanov, E. P. Ivanova, L. V. Knight, "Energy approach to consistent QED theory for calculation of electron collision strengths: Ne-like ions". Phys. Rev., Vol. 48, pp.4365-4377, 1993
9. L. N. Ivanov, E. P. Ivanova, "Method of Sturmian orbitals.in calculations of physical characteristics of radiation from atoms and ions", Zh. Exp. Theor. Fiz. Vol. 110, pp.483-498 (August, 1996).
10. E. P. Ivanova and I. P. Grant, "Effect of oscillator strength transfer and radiative decay cancellation in Ne-like and Ni-like sequences", Inst. Phys. Conf. Ser No 159. Paper presented at X-ray Laser Conf., Kyoto, 31 August – 4 September 1998, pp.395-399.
11. L. N. Ivanov, E. P. Ivanova, L. V. Knight, and A. G. Molchanov, "Spectrum of plasma containing Ne-like and Na-like ions: consistent accounting for Rydberg and autoionizing Rydberg series in balance equations", Physica Scrypta, V.53, pp.563-567, 1996.
12. E. E. Fill, "The radiation escape factor", J. Quant. Spectrosc. Radiat. Transfer, Vol.39, pp.489-491, 1988.
13. J. J. Rocca et. al., Phys. Rev. Let., Vol.73, pp.2192-96 (1994).
14. B. R. Benware, C. H. Moreno, D. J. Bird, J. J. Rocca, Optics Letter, Vol. 22, pp.796-99 (1997).
15. A. Hildebrand et. al., Inst. Phys. Conf. Ser No 151. Paper presented at X-ray Laser Conf., Lund (Sweden) 1996, pp.187-190.
16. E. P. Ivanova, N. A. Zinov'ev,, Gain calculation on Ne-like argon transitions in capillary discharge, Quantum electronics (Russian J), 1999 (in press).
17. T. Boehly, M. Russotto, R. S. Craxton, R. Epstein, B. Yaakobi, L. B. Da Silva, J. Nilsen, E. A. Chandler, D. J. Fields, B. J. MacGowan, D. L. Matthews, J. H. Scofield, G. Shimkaveg, "Demonstration of narrow-divergence x-ray laser in neon-like titanium", Phys. Rev. A, Vol.42, pp.6962-65 (1990).
18. J. Nilsen, B. J. MacGowan, L. B. Da Silva, and J. Moreno, "Prepulse technique for producing low-Z Me-like x-ray lasers", Phys. Rev. A, Vol.48, pp.4682-85 (1993).
19. Ph. Zeitoun, A. Mc.Phee, F. Albert, A. Carillon, P. Jaegle, G. Jamelot, A. Klisnick, M. Maillard, D. Ros, B. Rus, S. Sebban, C. L. Lewis., N. O'Rourke, J. Warwick, R. Smith, G. J. Tallents, "Obtention of high gains in the 3s-3p J=0-1 transition of Ne-like iron by an improved control of the ionization balance", Inst. Phys. Conf. Ser No 159. Paper presented at X-ray Laser Conf., Kyoto, 31 August – 4 September 1998, pp.115-118.
20. D. L. Matthews et al., Phys. Rev. Let., Vol.54, pp.110-115 (1985)

Downloaded From: http://proceedings.spiedigitallibrary.org/ on 03/27/2014 Terms of Use: http://spiedl.org/terms

21. M. D. Rosen et al., Phys. Rev. Let., Phys. Rev. Let., Vol. 54, pp.106-109 (1985).
22. E. P. Ivanova, and L. V. Knight, "Prediction of a large ASE effect in silver plasma produced by a short-pulse-drive laser', J. of x-ray science and technology, Vol.7, pp.339-347 (1997).
23. J. Zhang, A. G. MacPhee, J. Lin, E. Wolfrum, R.Smith, C.Danson, M. H. Key, L. S. Lewis L S, D. Neely, J. Nilsen, G.J. Pert, G. J. Tallents, J. S. Wark, *SCIENCE* , Vol. 276, pp. 1097-99 (1997).
24. J. Zhang, A. G. MacPhee, J. Nilsen, J. Lin, T. W. Jr. Barbee,, C. Danson, M. H. Key, C. L. S. Lewis, D. Neely, R. M. N. O'Rourke, G. J. Pert, R. Smith, G. J. Tallents, J. S. Wark and E. Wolfrum E, *Phys Rev Let* Vol. 78, 3856-58 (1997).
25. H. Daido, S. Ninomiya, T. Imani, R. Kodama, M. Takagi, and Y. Kato Y, *Optics Letters* , Vol. 21, pp. 958-961 (1996).
26. B. J. MacGowan, S. Maxon, P. L. Hagelstein, G. J. Keane, R. A. London, D. L. Matthews, M. D. Rosen, J. H. Scofield, and Whelan D A, *Phys.Rev.Lett.* Vol. 59 2157-60 (1987).
27. B. J. MacGowan, S. Maxon, C. J. Keane, R. A. London, D. L. Matthews and D. A.Whelan D.A. *J. Opt. Soc. Am.* Vol. B5, pp. 1858-62 (1988).
28. B. J. MacGowan, S. Maxon, L. B. Da Silva., D. J. Fields, C. J. Keane, D. L. Matthews., A. L. Osterheld, J. H. Scofield, G. Shimkaveg and G. F. Stone, *Phys.Rev.Lett.* Vol. 65, pp. 420-425 (1990).
29. S. Maxon, P. L. Hagelstein, J. H. Scofield , and Y. J. Lee, *J. Appl. Phys.* Vol. 59, pp. 239-243 (1986)..
30. S. Maxon, S. Dalhed, P. L. Hagelstein, R. A.London, B. J. MacGowan, M. D. Rosen, G. Charatis and G. Bush, *Phys. Rev. Let.* Vol. 63, pp. 236-240 (1989).
31. S. Maxon, K. G. Estabrook, M. K. Prasad, A. L. Osterheld, R. A. London, and D. C. Eder, *Phys. Rev. Let.* Vol.70 pp.2285-89 (1993).

Downloaded From: http://proceedings.spiedigitallibrary.org/ on 03/27/2014 Terms of Use: http://spiedl.org/terms